 doi:10.20944/preprints202207.0162.v1

Article

Association of circular RNA and Long Noncoding RNA dysregulation to clinical Response to Immunotherapy in Cutaneous Metastatic Melanoma.

Javier Oliver[*1], Juan Luis Onieva[*1,2], María Garrido-Barros[1,2] ,Miguel Berciano-Guerrero[1], Alfonso Sánchez[1], María José Lozano[3] Angela Farngren[4], Martina Álvarez[1,3], Beatriz Martínez-Gálvez[1], Elisabeth Pérez-Ruiz[1], Emilio Alba[1], Manuel Cobo-Dols[1], Antonio Rueda-Dominguez[#1], Isabel Barragán[#∞1,4]

*# Equal contribution

1 Medical Oncology Intercenter Unit; Regional and Virgen de la Victoria University Hospitals; IBIMA; 29010; Malaga; Spain, Cancer Molecular Biology Laboratory (LBMC); Health and Medical Research Centre (CIMES); University of Malaga (UMA); Marques de Beccaria 3; 29010; Malaga; Spain, Institute of Biomedical Research in Malaga (IBIMA); 29010; Malaga; Spain.

2 University of Málaga, 29010, Málaga, Spain.

3 Anatomy-Pathology Department, University of Málaga, 29010, Málaga, Spain.

4 Group of Pharmacoepigenetics, Department of Physiology and Pharmacology, Karolinska Institutet, Stockholm, Sweden

∞ Correspondence: Isabel Barragan; isabel.barragan@ibima.eu; 0034658987896.

Abstract: Cutaneous Melanoma (CM) is the most lethal form of skin cancer if it becomes metastatic, where treatment options and survival chances decrease dramatically. Immunotherapy treatments based on the immunologic checkpoint inhibitors (PD-1 and CTLA4) constituted a main breakthrough in the treatment of metastatic CM, particularly in the long-term benefit. However, several molecular pathways are responsible for the failure of this strategy in about 50-70% of CM patients. Some Long Non-coding RNAs (lncRNAs), and circular RNAs (circRNA) are implicated in triggering pro- and antitumorigenic responses to various cancer treatments. The relationship between lncRNA, circRNA and Immune Checkpoint Blockade (ICB) immunotherapy is not extensively explored in cutaneous metastatic melanoma (CMM). The aim of this study is to evaluate the potential role of both circRNA and lncRNA as a predictive immunotherapy biomarker in CMM. RNA-seq from 12 FFPE samples from the metastatic biopsy of metastatic melanoma patients treated with Nivolumab were analyzed. Our findings indicate that specific lncRNA and circRNA are involved in regulatory networks of the immune response against metastatic melanoma under treatment with nivolumab. Moreover, we have established a risk score that allows the prediction of Overall survival (OS) and Progression-free survival (PFS) of CMM patients with high accuracy. This proof of principle work provides a possible insight on the function of ceRNA, contributing to decipher the complex molecular mechanism of ICB cancer treatment response.

Keywords: Circular RNA, Cutaneous Melanoma, Immunotherapy, metastasis, LncRNA, ecRNA

 doi:10.20944/preprints202207.0162.v1

1. Introduction

Melanocytes are pigment-producing cells in the skin embrionary-derived from the neural crest [1] Epidermal melanocytes can undergo a malignant tumor transformation process that leads to Cutaneous Melanoma (CM), which is the deadliest type of skin cancer [2]. CM is a common cancer with increasing incidence rates in the western world [3]. In 2040, 510000 new cases are expected to be diagnosed; of them, it is calculated that around 96000 will die [3–5]. Both genetics and environmental risk factors have been characterized for CM. Exposure to ultraviolet radiation (UV) is the main risk factor for melanoma. UV radiation is known to generate mutations that induce cell death and malignant transformation of melanocyte cells [6]. One of the consequences of the constant exposure to UV is that melanoma has one of the highest mutation rates and mutational burdens compared to other solid malignancies [7]. Genomic studies have identified several driver genes in melanoma such as *BRAF, NRAS, TP53, PTEN,* among others, as well as the relevant pathways involved in its carcinogenesis like the CDKN2A, MAPK and PI3K/AKT pathways, and the cell cycle control and telomerase programs. All of them are affected by pathologic somatic mutations in protein-coding genes [8].

Interestingly, many of these mutations arise early in the clinical process; for example, over 80% of benign nevi have already a *BRAF* mutation [9]. In more advanced stages, metastatic progression is driven by specific genomic alterations including somatic mutations and other perturbations of the genomic integrity [10,11].

Detected and treated early on, CM is highly curable. However, if CM becomes metastatic, treatment options and survival chances decrease dramatically. Immunotherapy treatments based on the immunologic checkpoint inhibitors PD-1 and CTLA4 have been a main breakthrough in the treatment of metastatic CM and have changed the landscape of treatment options for CM in the recent years [12]. Even though it is a very promising therapy, primary immune checkpoint blockade resistance arises in about 70% of CM patients treated with a CTLA-4 inhibitor and 40–65% of CM patients administered with PD-1-targeting treatment[13,14]. Several studies have proposed a variety of molecular pathways that might lead to therapy failure [14,15]. There is currently a great effort trying to determine reliable biomarkers for predicting immunotherapy response, among which the predominant ones are PD-L1, microsatellite instability and TMB. To present, only tumor mutational burden (TMB) has been tested as a biomarker in therapeutic trials, but it has not been found to predict clinical benefit in melanoma patients, owing to the high mutation rate of all melanoma tumors [14,16].

A wide range of distinct RNA species have recently been spotlighted thanks to the advent of RNA sequencing (RNA-seq). Non-coding RNAs (ncRNAs), which comprise 98 percent of the human genome, are implicated in triggering pro-tumorigenic and anti-tumorigenic responses to various cancer treatments [17]. Of them, two particular RNA species have lately sparked interest in different disciplines including cancer research: Long non-coding RNAs (LncRNAs) and Circulating RNAS (CircRNAs). CircRNAs are single-stranded stable RNAs that are produced by covalently closing head-to-tail (or back-spliced) circularized transcripts from 5′-to-3′ transcription of coding gene exons or long non-coding RNAs (lncRNAs). CircRNAs have been linked to a variety of biological functions, including protein translation templates, RNA-binding protein regulators, and miRNA-binding sponges, among others. Several circRNAs are also involved in tumor regulation in a variety of malignancies[18]. CircRNAs have been found to interact with miRNAs and create a network to control cellular physiological and pathological functions in several scenarios [19]. In melanoma, several circRNAs such as CDR1-AS [20] , circ_0002770 [21] circRNA_0084043 [22,23], circ_0025039 [24], circ-MYC [25], circ_0079593 [26], circ-FOXM1[27], circ_0020710 [28] work as miRNA sponges or interact with RBPs to modulate the expression level of target miRNAs or proteins, which in turn affects various cellular signaling cascades and cancer-related cellular transitions [29–31].

The LncRNAs are defined as noncoding RNA molecules longer than 200 nucleotides. An increasing amount of data suggests that LncRNAs have a variety of roles in cellular

 doi:10.20944/preprints202207.0162.v1

activities notwithstanding that they are not translated into proteins. LncRNA can interact to control gene expression by altering local chromatin structure or recruiting regulatory molecules to particular locations [30]. While the interactions with proteins can either promote or inhibit protein complexes formation, the interactions with mRNAs can be more intricate and alter their stability, translation, and isolation [32]. Regarding the expression levels of lncRNAs, it is important to note that even though they are expressed at lower levels than protein-coding genes, they have marked tissue-specific expression patterns[33] Both lncRNAs and circRNAs can be acting as competitive endogenous RNAs (ceRNAs) [34] and lead to a new additional posttranscriptional layer. The ceRNA hypothesis argues that biological processes are regulated by an intrinsic mechanism. It is becoming increasingly apparent that dysregulated of lncRNA and circRNAs are implicated in carcinogenesis and progression of numerous cancers, acting as either oncogenes or tumor suppressors [30]. Moreover, abnormal circRNAs levels have been shown to be associated with the development of resistance of chemotherapy in different tumors [35]. However, to our knowledge, the relationship between lncRNAs and circRNAs and ICB immunotherapy has not been explored in cutaneous metastatic melanoma. With all these, the aim of this study is to evaluate the potential role of circRNA and lncRNA expression as predictive immunotherapy biomarkers in CMM.

2. Materials and Methods

Subjects

A total of 16 metastatic melanoma patients treated with Nivolumab donated FFPE biopsy samples that were collected at pre-treatment status (four samples derived from primary tumors biopsy and twelve from metastatic tissue). Samples were collected at the Hospital Regional de Malaga and Hospital Universitario Virgen de la Victoria (Málaga). The study follows the Declaration of Helsinki and is vetted by the Ethical Committee of Malaga. Approval date on 26/10/2017 with the title: "Omics integration for precision cancer immunotherapy" (799818, H2020-MSCA-IF-2017) research project. All patients signed an Informed Consent to participate in the study and received an information sheet about the project.

For this specific analysis, we used the metastatic biopsies in order to identify biomarkers that were specific to the metastatic disease, giving the scarce knowledge in the field [36] and this it is currently the most frequent indication for immunotherapy in melanoma.

Bad responders were defined as patients that progressed up to three months after the start of the treatment and good responders were the ones in treatment for at least one year.

Nucleic acid extraction

The tumor-specific area in FFPE melanoma samples was predefined by a pathologist. Two to four 10 μm slides were dissected for nucleic acid extraction, using the microtome HM 340E (Thermo Scientific). RNA was extracted with the RNeasy FFPE kit (Qiagen; Ref. 73504).

Next Generation Sequencing

RNA-Seq libraries were prepared using TruSeq Stranded Total RNA Gold (Illumina; Ref.20020598) and indexed by IDT for Illumina TruSeq RNA UD Indexes (Illumina; Ref. 20020591). Libraries concentration was determined by Qubit dsDNA BR kit, and the size distribution was examined by Agilent Bioanalyzer. Paired end reads (75bp × 2) were acquired from the Illumina NextSeq 550 platform according to the corresponding protocol.

 doi:10.20944/preprints202207.0162.v1

Realtime PCR validation

The expression levels of CDR1-AS the most frequent circRNAs was verified by qRT-PCR using a predesigned TaqMan probe in all samples. (Hs05016408_s1).

lncRNA and circRNA detection

Quality control of Fastq data from pair end reads was performed with FastQC. Fastq files were trimmed with a cutoff of Q30. We evaluated five different pipelines to identify and quantify circRNA reads. CIRI[37], CIRCExplorer2[38], DCC[39], STARchip[40] and CIRI-QUANT[41] were used and compared. The circRNA sequences were annotated based on the circAtlas 2.0 database [42]. To obtain high confidence circRNAs, we used a filtering cut-off minimum of two junction reads in at least two samples and in at least three software (validation strategy), which allowed a minimum of back-splice junction reads (BSJ) per circRNA. This criterion resulted in 19030 unique circRNAs in all samples, and we used these high confidence circRNAs for all the analyses performed in this study. With forward-splice junction reads (FSJs) and back-splice junction reads (BSJs), we used the following formula: 2*bsj/(2*bsj+fsj) to calculate the circular to linear transcripts ratio. LncRNAs reads were identified by mapping trimmed fastq files against reference genome GRGh38 using STAR (v 2.5.1b). Read quantification was done with Feature Count. LncAtlas[43] was used to annotate lncRNAs.

Differential expression analysis

The DESq2 pipeline of total mapped reads were used to perform differential expression (DE) of high confidence circRNA and lncRNA. The differential expression analysis was based on negative binomial generalized linear models and the threshold values were adjusted p-value < 0.1 and absolute value of log2(fold change) > 1.5. For both circRNA and lncRNA DE analysis, the total linear mapped read counts were used for size factor estimation.

ceRNA- miRNA-mRNA interactions

Analysis of Common Targets for circRNAs (ACT) [44] , which employs miRbase [45] and miRanda [46] , was used to identify miRNA-binding sites for the differentially expressed circRNAs. To characterize lncRNAs and get the list of miRNAs: DE lncRNA interactions, DIANA-LncBase v2 [47] was employed. The R multiMir package[48] was used to detect the microRNA-mRNA interaction. This package combines up to seven different tools: DIANA-microT, ElMMo, MicroCosm, miRanda, miRDB, PicTar, PITA, and TargetScan [49–56]. To improve prediction sensitivity, only those interactions that appear in at least 5 different tools will be considered as a microRNA-mRNA pair. Only differentially expressed mRNAs with a binding site with a miRNA from the joint combination of miRNAs obtained from DE circRNA and DE lncRNA were considered for the analysis.

We also compared our deferentially expressed circRNAs to those reported in prior research using the circRNA disease databases circ2disease [57], circad [58], and circAtlas [42]. The CSCD database [59] was used to estimate cellular localization of all detected circRNAs.

Pearson correlation coefficient was used to measure the strength of the linear association between ceRNA and mRNA.

Gene Set Enrichment and Gene Interactions Networks

Preprints (www.preprints.org) | NOT PEER-REVIEWED | Posted: 11 July 2022 doi:10.20944/preprints202207.0162.v1

DE mRNA genes targeted by predicted miRNAs were analyzed using Ingenuity Pathways Analysis (IPA) software (Qiagen Ingenuity Systems; (www.ingenuity.com/). Upstream regulator analysis (URA), downstream effects analysis (DEA), mechanistic networks (MN), and causal network analysis (CNA) prediction algorithms were used to get functional annotations and regulatory network analysis. IPA can precisely predict functional regulatory networks from gene expression data and assigns a significance score to each network based on how well it fits the database's set of focus genes [60].

Statistics and Visualization

Statistical analyses chart and graphs were performed using R 4.0.2. The Venn Diagram R package was used to create Venn diagrams. The ComplexHeatmap R package [61] was used to create the heatmaps, and the subsequent plots and graphs were created with the ggplot2 package [62]. In survival analysis, Kaplan–Meier (KM) and Logrank-test were used to test the difference between groups. The risk score for each patient was estimated adapting the previously described method for the estimation using the joint expression information of the circRNA and the lncRNA [63]. Based on the expression value of circRNA and LncRNA weighted by regression coefficients in univariate cox regression analysis

$$\text{Risk Score (RS)} = \sum_{i=1}^{N} (\text{Expression}_i * \text{Coefficient}_i)$$

Where N is the number of DE circRNA and lncRNA, Expression-i represents the normalized expression value, and Coefficient-i is the Cox regression coefficient in the univariate model

3. Results

3.1 Overview of circRNA and lncRNA expression patterns in cutaneous melanoma tissues

We analyzed the circRNA and lncRNA transcripts by RNA-seq sequencing analysis with rRNA depletion from FFPE tissue of clinical metastatic cutaneous melanoma tumors to find aberrant expression of these ceRNAs between good and bad responders to ICB. The raw sequences were processed with five different circRNA pipelines to increase the analysis specificity and sensibility. Only circRNAs that were found in at least three of the five pipelines were selected for further analyses (19030 circRNAs). Both differentially expressed (DE) circRNA and DE lncRNA between good and bad responders were used to build a ICB-response ceRNA network (**Figure 1a)**. Overall, 4339 circRNA loci were detected by all tested software in metastatic tissue samples (**Figures 1b** and **1c**). The top ten circRNAs generating loci were *hsa-CDR1*, *hsa-HIPK3*, *hsa-SMARCA5*, *hsa-CSNK1G3* and *hsa-PCMTD1*. Interestingly, *hsa-CDR1* stands as the top circRNAs loci with remarkable distances to the others in 4 out of the 5 software. Moreover, the pattern of enrichment in bad responders is reproduced by all 5 (**Figure 2a**). The distribution of circRNAs according to response throughout the 46 human chromosomes indicates a similar horizontal coverage between good (yellow line) and bad (blue line) responders (**Figure 2b**) However, some chromosomes such as 1, 5, 8 ,18 and 22 are enriched in circRNAs for bad responders. Interestingly, irrespective of the distribution by response, the total number of reads did not correlate with the chromosomal length. This is particularly patent in chromosome 3 and 12 (**Figure 2C**). Remarkably, the most significant entity was circRNA derived from protein coding regions (supplementary figure 1).

Preprints (www.preprints.org) | NOT PEER-REVIEWED | Posted: 11 July 2022 doi:10.20944/preprints202207.0162.v1

Figure 1. 1a) Bioinformatic workflow of the ceRNA interaction network. The pipeline is depicted from the RNA-seq fastq files to the Ingenuity Pathway analysis. Five different software were employed to identify circRNAs. mRNAs affected by ceRNAs were predicted by its interaction with miRNA. Differential expression analysis with DESeQ2 was used to decipher differences in response to immunotherapy. **1b)** Venn diagram with the number of different cirRNAs detected by each software. **1c)** Upset plot showing the maximum number of identified circRNA with each software combination.

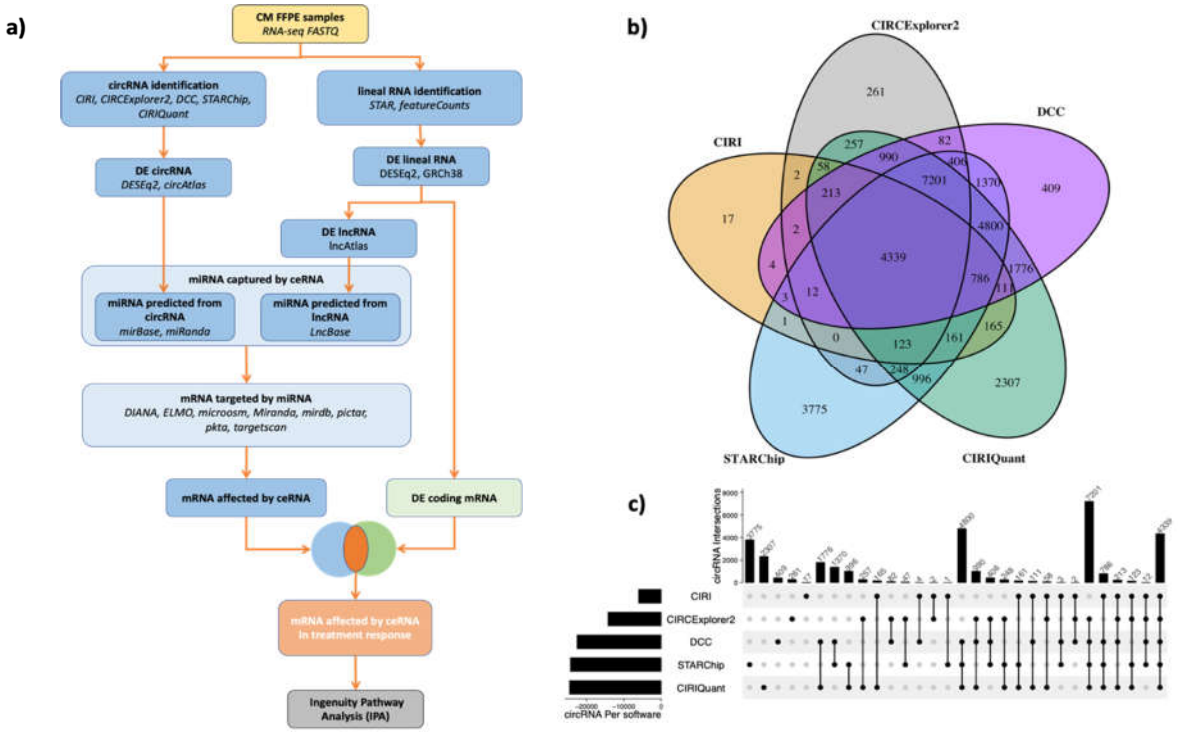

Figure 2. Frequencies and distribution of the circRNAs by response to ICB 2a) Top 10 circRNA loci identified by the different algorithms used. **2b**) Horizontal chromosomal coverage. **2c)** Normalized count quantification per chromose.

a)

Preprints (www.preprints.org) | NOT PEER-REVIEWED | Posted: 11 July 2022 doi:10.20944/preprints202207.0162.v1

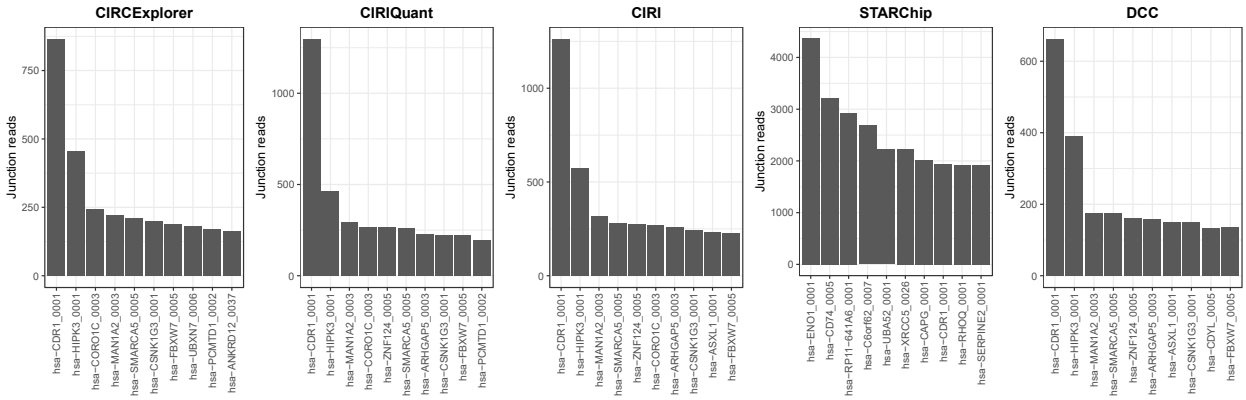

b)

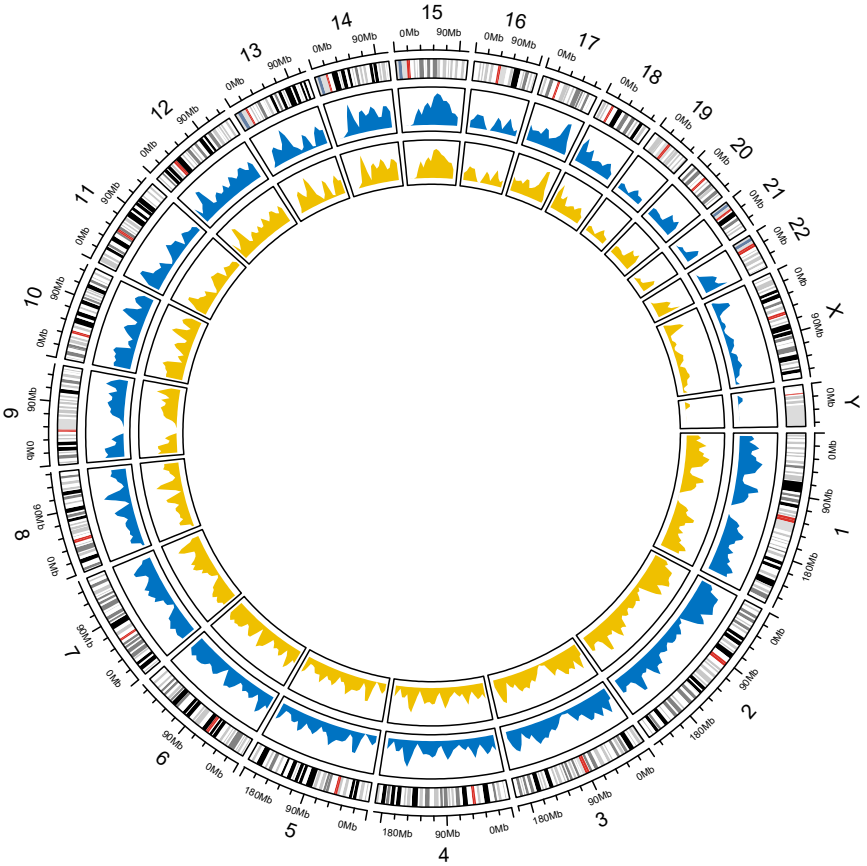

c)

Preprints (www.preprints.org) | NOT PEER-REVIEWED | Posted: 11 July 2022 doi:10.20944/preprints202207.0162.v1

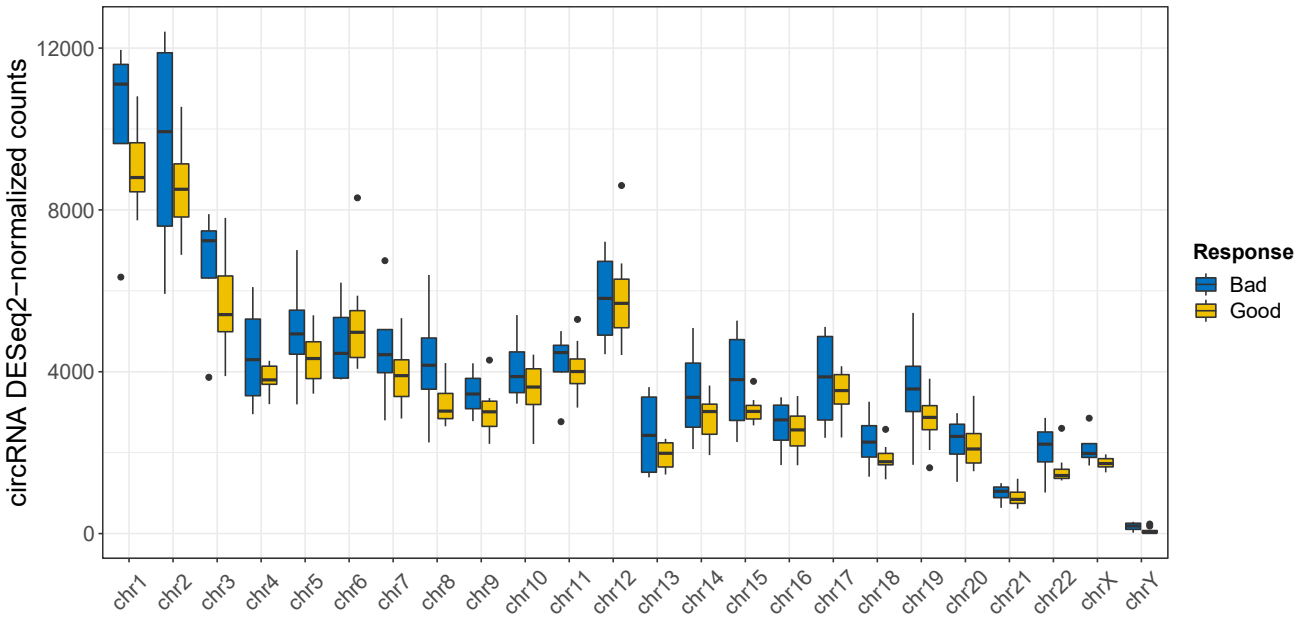

3.2 Differential Gene Expression of circRNA and lncRNA

To analyze the expression pattern of lncRNA and circRNA in relation to response to immunotherapy, we identified the expression profile of dysregulated circRNAs and lncRNAs in 8 good versus 4 bad responders using whole genome transcriptome analysis. In the volcano map, we depict the differentially expressed circRNAs (**Figure 3a**) and lncRNA (**Figure 3b)** with a fold-change cut-off greater than 1.5 and an adjusted p value less than 0.1. We found 23 aberrantly expressed circRNA with a fold change of > 1.5 and adjusted p value < 0.1, of which 21 circRNA were upregulated and only two were down-regulated. To further characterize the identified DE circRNA, we retrieved data from three circRNA databases: circBase, circAltlas and Cancer Specific CircRNA Database (CSD). The annotations from CSD, a circRNA database focused on cancer, were particularly relevant, where we found 15 circRNAs (68.2%). On the other hand, 7 of the 23 DE circRNAs (31,8%) were newly identified in this study. Based on the fold change, the top five most upregulated circRNA were *hsa-ALDH1L2_0014*, *hsa-CD38_0001*, *hsa-CD74_0005*, *hsa-CDR1_0001* and *hsa-CPM_0002*.

To better understand the relation between linear and circular expression seeking other possible differences between good and bad responders, we have determined the circular-linear ratio of the differentially expressed circRNAs (**Figure 3 c).**. The inferred ratios from RNAseq data with the formula 2* Circular/(2*Circular + Linear), showed a broad distribution of ranges from 0.1 to 1. This analysis can represent the splicing preference of the loci interrogated. We observed ratios higher than 0.5 in hsa-SLIT2, has-RP11, hsa-IFI30, hsa-HLA-DRB1 and hsa-CDR1. Interestingly, hsa-CDR1 shows one of the higher ratios and is the most relevant circRNA, in term of number of counts, it is transcribed with a total of 2211 counts distributed in 1644 vs 567 counts between good and bad responders, respectively.

Regarding LncRNA, 112 were differentially expressed with a fold change of 1.5 and adjusted p value < 0.1, from which 58 were found downregulated and 54 upregulated. DE lncRNA were annotated with LncAtlas[43].

Preprints (www.preprints.org) | NOT PEER-REVIEWED | Posted: 11 July 2022 doi:10.20944/preprints202207.0162.v1

Finally, we were able to group good and bad responders by their basal expression of circRNA and lncRNAs. Hierarchical clustering analysis showed good discrimination among good and bad responders for both types of RNAs (**Figure3d** and **3e**).

Figure 3. CeRNAs as biomarkers of response to ICB in metastatic melanoma 3a) X circRNAs are differentially expressed (LFC X p value X) **3b)** X lncRNAs are differentially expressed (LFC x value x) **3c)** Ratio of circRNA vs lineal RNA per DE circRNA loci. Y-axis list the DE circRNA among good and bad responders. X-axis represent ratio : 2*circular/(2*circular+linear) were range 0 represent deviation to linear expression and 1 maximun deviation to circRNA expression . EXPLICA LA GRÁFICA **3d)** & **3e)** Expression signatures of the DE circRNAs and DE lncRNAs, respectively, separate good and bad responders to ICB. Normalized expression values are represented against location and several clinical variables.

a)

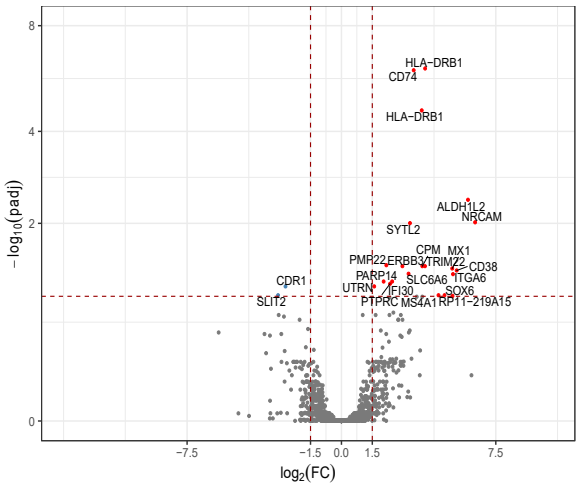

B)

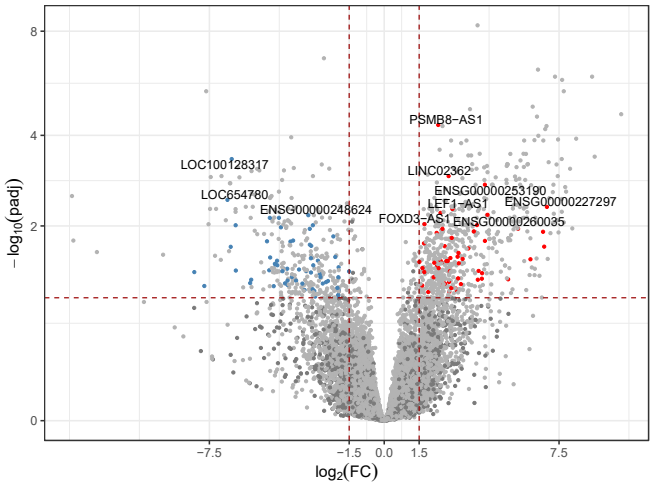

c)

Preprints (www.preprints.org) | NOT PEER-REVIEWED | Posted: 11 July 2022 doi:10.20944/preprints202207.0162.v1

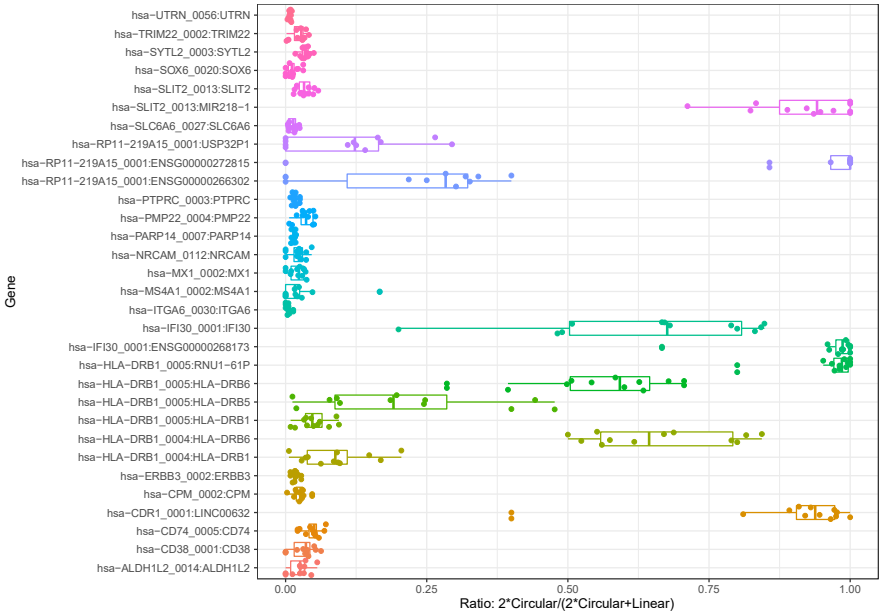

d)

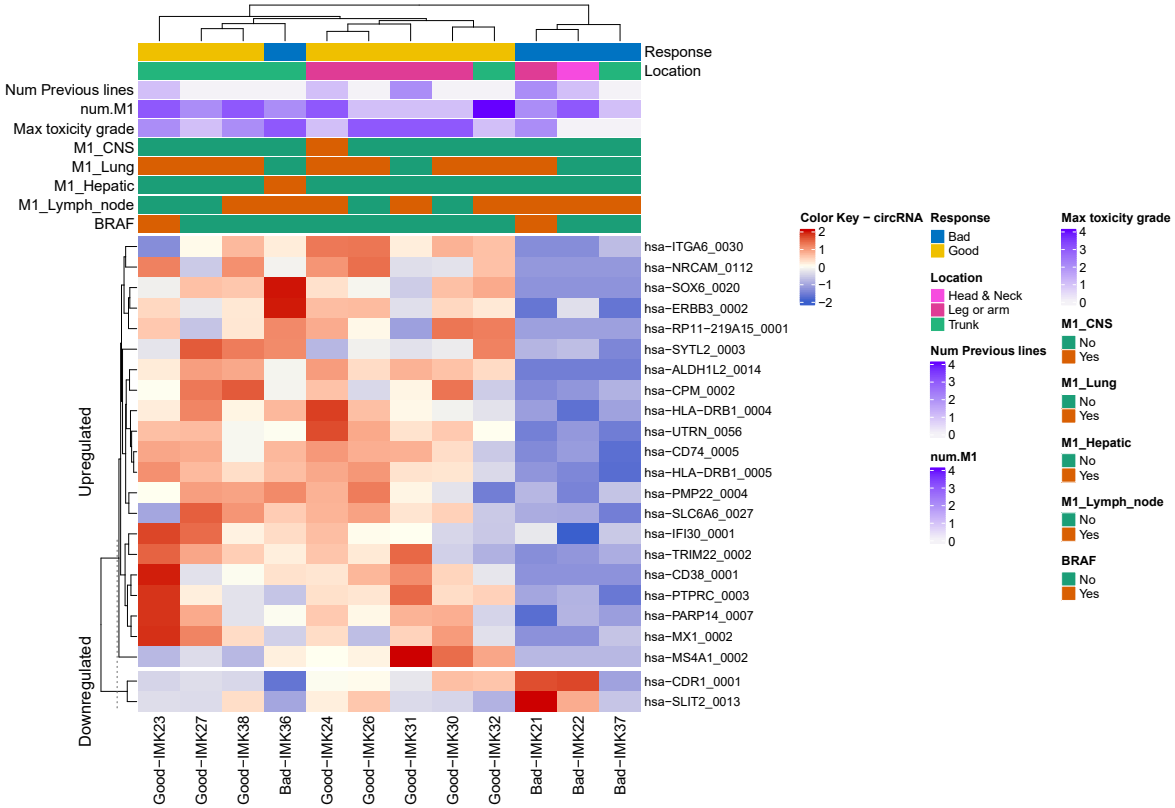

e)

Preprints (www.preprints.org) | NOT PEER-REVIEWED | Posted: 11 July 2022 doi:10.20944/preprints202207.0162.v1

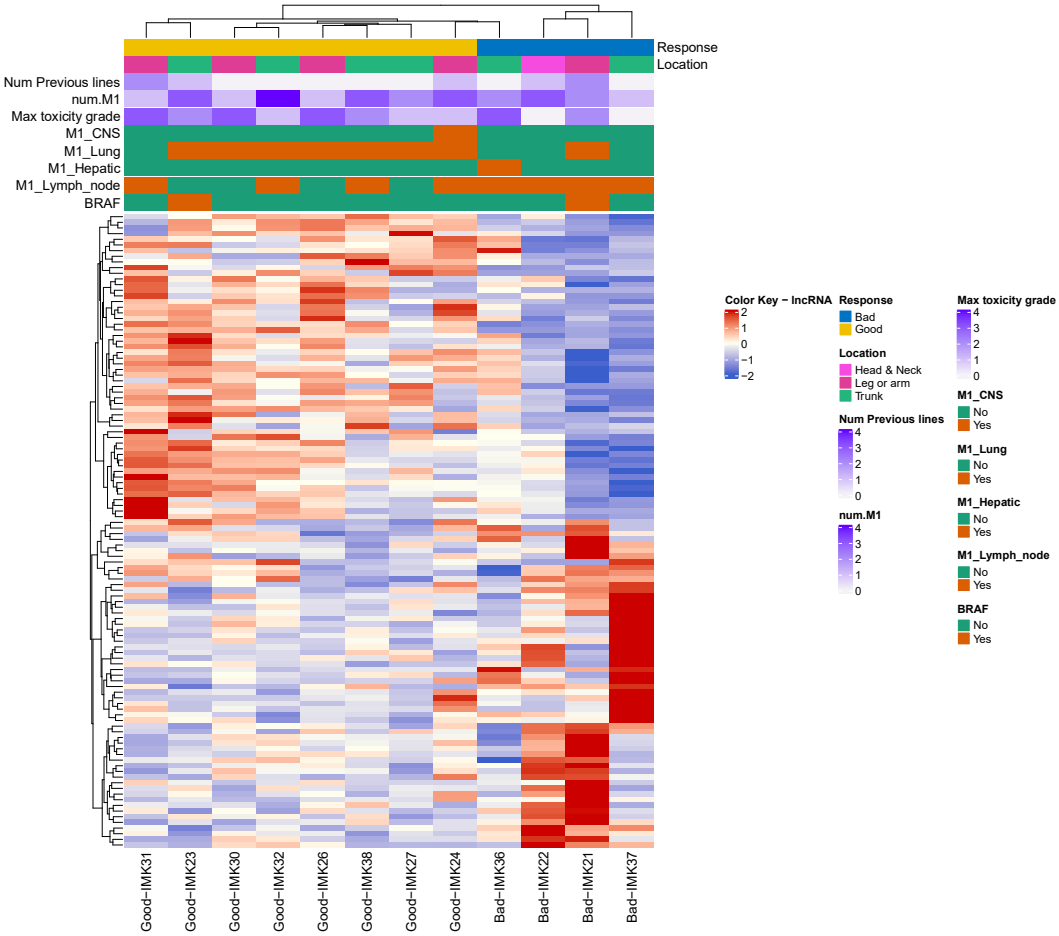

3.3 Competitor endogenous RNA network (ceRNA Network)

In order to understand the role of the DE circRNAs and lncRNAs as posttranslational regulators in the context of resistance to ICBN, a ceRNA Network was build that included 69 lncRNA (36 upregulated and 33 downregulated; the 43 missing lncRNAs up to the total 122 DE lncRNAs do not have any miRNA interaction) and 23 circRNA, (21 upregulated and 2 downregulated). Two additional layers complemented the network. One of them consisted of 537 target miRNAs, from mirBase with strongly predicted binding sites to our DE circRNAs and lncRNAs. Of them, the ones showing the highest prediction values were *Let-7e-5p*, *miR-1285-3p*, *miR-6757-3p*, *miR-877-3p*, and *miR-3689d*. The second additional component comprised 154 DE mRNAs among good and bad responders that showed interaction with miRNAs predicted to bind the DE ceRNAs. Furthermore, the statistical correlation between the DE mRNAs regulated by these miRNAs and the DE ceRNAs shows that all correlations are direct, reinforcing the notion of the ceRNA inhibitory role on miRNAs action (**Figure 4**). We have also identified several major putative regulators such as *LINC00861*, *CHRM3-AS2*, *MEG3* and *RP11−115D19.1*, which correlated with multiple mRNAs, as well as 3 mRNAs that we speculate can be regulated by 2 or more ceRNAs in the context of melanoma resistance to Nivolumab: *ICOS, PAX3, HLA−DOA* and *HLA−DPB1*.

Figure 4. Lineal correlation of expression of the DE ceRNAs and the DE mRNAs that belong to the ceRNA interaction network.

Preprints (www.preprints.org) | NOT PEER-REVIEWED | Posted: 11 July 2022 doi:10.20944/preprints202207.0162.v1

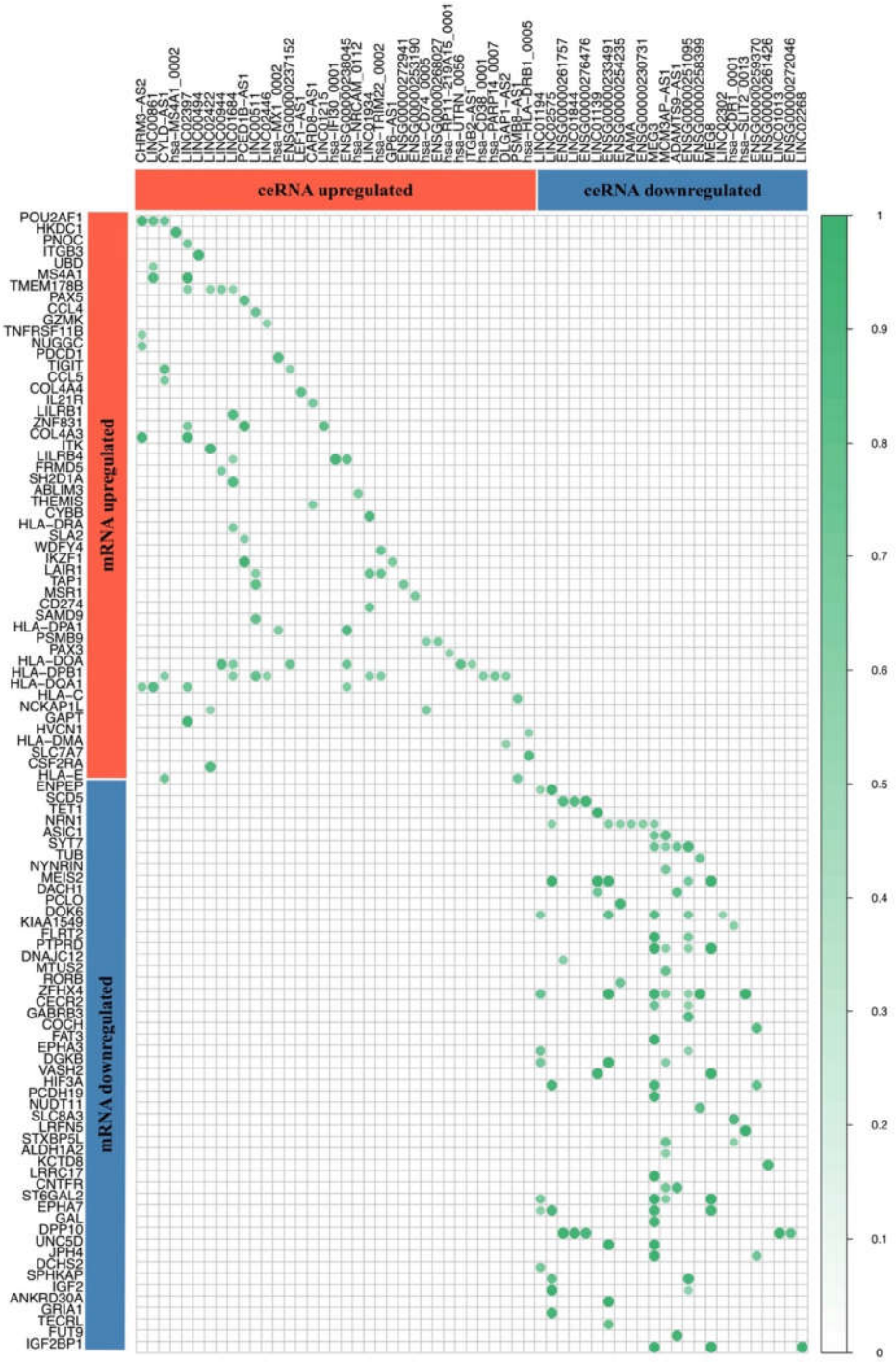

3.4 IPA Functional Enrichment Analysis based on the ceRNA Network

Preprints (www.preprints.org) | NOT PEER-REVIEWED | Posted: 11 July 2022 doi:10.20944/preprints202207.0162.v1

In order to gain more quantitative and qualitative insight into the mechanism of the putative regulation of ICB response by ceRNAs, we characterized the biofunctions and the diseases associated with those DE mRNA that interacted with the DE ceRNA, as well as the downstream and upstream modulators. Influence network analysis shows that the differential expression of the interactome key molecules led to activity changes mostly in immunological processes. Activated molecules include TNF, IRF, IL27, TLR9, EIB3, TGM2 and IFNG, an inhibited ones include MAPK1 and IL1RN (**Figure 5a**). In the same line almost all the enriched functional categories are related to the immune response, and even specifically to the PD-1 PD-L1 cancer immunotherapy pathway, target axis of Nivolumab (**Figure 5b)**. Amongst the most activated functions in good responders are TH1 Pathway, T cell receptor signaling, ICOS-ICOS-L signaling in T Helper cells, Role of NFAT in Regulation of the Immune Response, Dendritic Cell Maturation, and calcium induced T lymphocyte apoptosis.), together with MSP–RON Signaling in Macrophages Pathway, Natural Killer Cell Signaling, and Synaptogenesis Signaling Pathway. The most relevant molecules annotated for these molecular functions are *CCL5*, *CD6*, CSF2RA, *HLA-B HLA-DRA*, HLA-E, *ICOS*, IKZF1, *IL12RB1*, *IL12R*, LAIR1, *LILRB2*, *LILRB4*, *MS4A1*, *PDCD1*, *TBX21* and *UBD*. It is important to note that key genes for the antitumoral immune response part of the PD−1 PD−L1 axis such as those coding for the receptor of TNF (TNFR), IFNγ, MHC1α and β and PD1 are upregulated in good responders to Nivolumab (**Figure 5c**).

Figure 5. Specific immunological perturbation associated to the ceRNA network 5a) Influence network showing the activation or inhibition of the key molecules and pathways defined by the ceRNAs 5b) Pathways enriched and influenced by the ceRNAs dysregulation according to response to ICB. **5c)** Activated and inhibited genes and pathways of the PD1-PDL1 axis in the context of ceRNA dysregulation.

a)

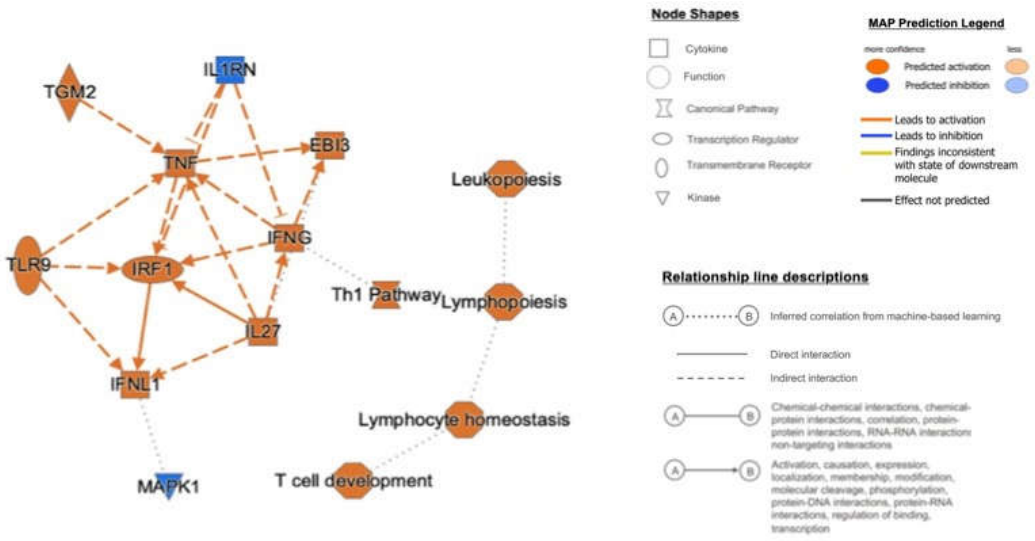

Preprints (www.preprints.org) | NOT PEER-REVIEWED | Posted: 11 July 2022 doi:10.20944/preprints202207.0162.v1

b)

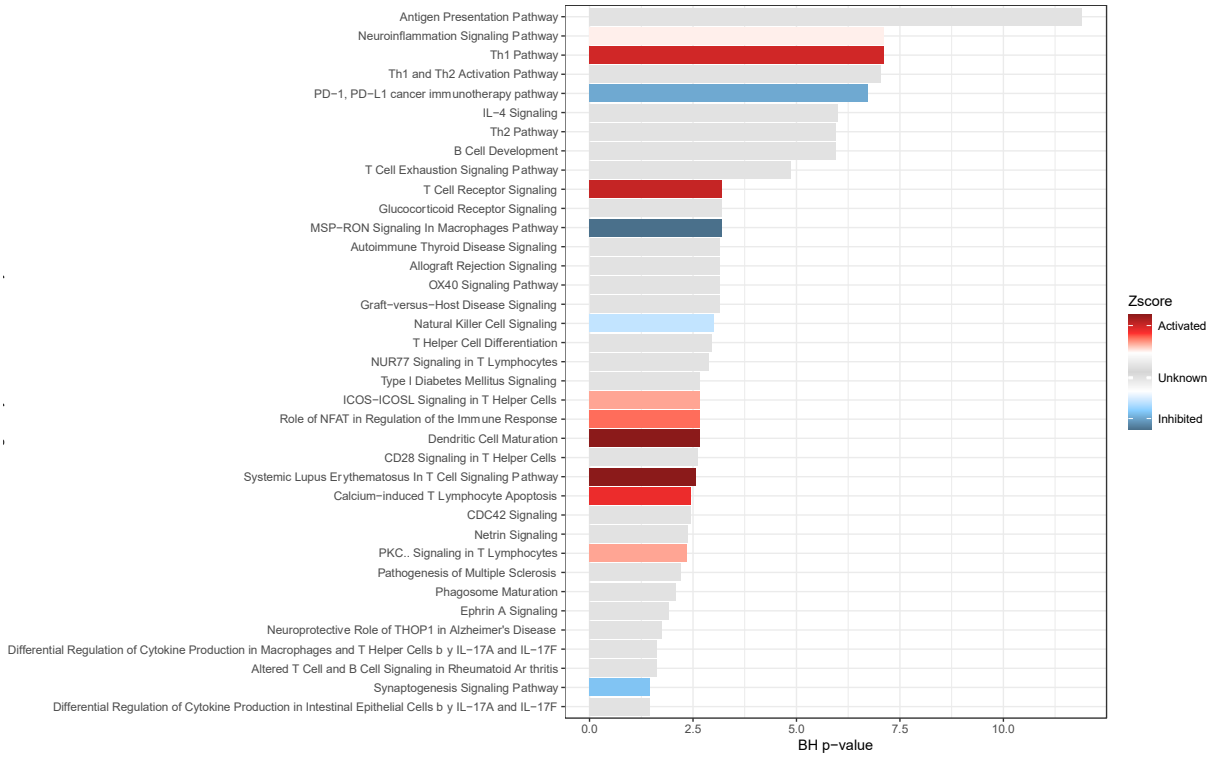

c)

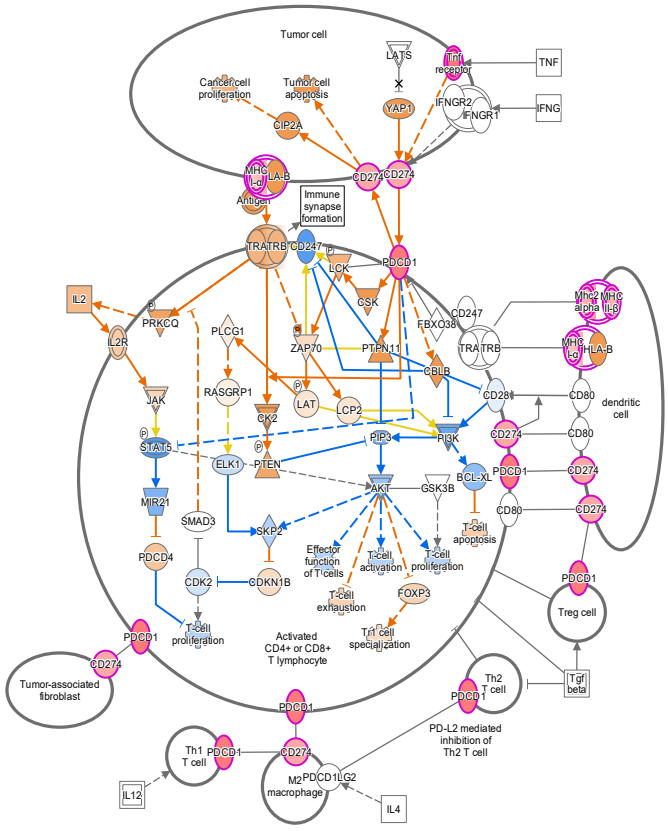

Preprints (www.preprints.org) | NOT PEER-REVIEWED | Posted: 11 July 2022 doi:10.20944/preprints202207.0162.v1

Next, by using the IPA upstream regulator analysis tool based on the ceRNA network, we can predict upstream molecules and provide a mechanistic network that could explain the observed changes in gene expression. Interestingly, we observed the following activated transcription regulators: SOX11, IRF1, NLRC5, and SMRACA4. NEUROG1 was found uniquely inhibited. Regarding cytokines, IL1RN and IL13 were inhibited and IL27, IFLN1, TNF, IFNG and EBI3 were predicted as activated. Other activated upstream regulators were TLR9 and TGM2, that were activated, and SAFB, SAFB2, RARA and ESR1 that were found inhibited.

Furthermore, to characterize the specific role of ceRNAs in the regulation of the mechanism of resistance to ICB, we sought to identify the pathway aberration related specifically to response genes that are correlated with such regulators. For this, we generated z-scores of IPA canonical pathways of all differentially expressed genes (DEmRNA) vs the DEmRNA correlated with ceRNAs (DEmRNA-ceRNA) and vs the differentially expressed genes not associated with ceRNA (DEmRNA-noceRNA) (**Figure 6**). It is very important to note that there are three pathways that denote an opposite activation profile compared with all or non-ceRNA related genes. One of them is *natural killer cell signaling*. Also, the Z-score of *PD–1, PD–L1 cancer immunotherapy* is lower when the pathway is defined by the expression differences of the genes related to ceRNAs. Moreover, ceRNAs seem to be involved in a fraction of the mechanisms associated to the drug response. This indicates that ceRNA may modulate specific processes of ICB resistance independently of other regulators that they can synergize or oppose.

Figure 6. Role of ceRNA as modulators of the ICB resistance. Comparison of the pathways aberration according to absence or presence of genes associated with ceRNAs.

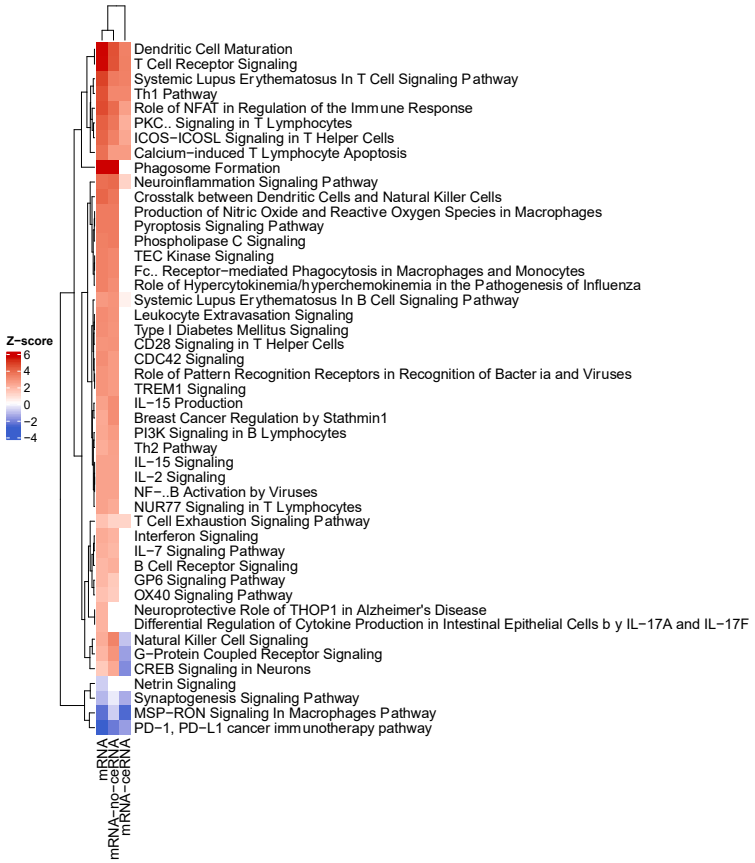

 doi:10.20944/preprints202207.0162.v1

When we extended the IPA network analysis by combining the main subnetworks, more than 100 molecules conformed a very complex interaction network where TNF emerges as a key functional molecule. Interestingly, individual networks also pinpoint the relevance of NR3C1, IFNG, CTNNB1, JUN, and the inhibition of the IL2 (**Supplementary Figure 2**).

Moreover, the gene ontologies and pathways were determined with IPA. The statistical overrepresentation test was used to find the enriched GO terms and pathways by matching our gene list with the human genome. The most relevant biological processes were: leukopoiesis, lymphopoiesis, cell development and lymphocyte homeostasis (GO:0002521, GO:0030098, GO:0046650, GO:0002260). **Supplementary Figure 3** represents the top enriched ontologies for Disease and disorders, Molecular and cellular function, and Physiological system & physiology. The enriched ontology terms were mainly related to cancer, cellular growth and cellular proliferation and immunological conditions. The most enriched Molecular and cellular functions were cellular development, cellular growth and Cell-to-Cell signaling and proliferation and the most enriched Physiological system were hematological system development and function, Lymphoid tissue structure and development and Immune cell trafficking. Like the GO term results, KEGG pathway enrichment analysis identified Axon guidance, T cell receptor signaling pathway, Natural killer cell mediated cytotoxicity, ErbB signaling pathway and Fc epsilon RI signaling pathway as the enriched pathways in the interactome (**Supplementary table 1**).

3.5 Prognostic risk score using the DE ceRNA

A risk score based on the gene expression of DE ceRNA categorized the patients in two groups: High and low risk. Patients with low risk have greater overall survival (OS), log-rank p-value 0.00018. The low-risk patients median OS was of 869 days (95% CI, 563 - NR) while patients with high risk have a median OS of 56 days (95% CI, 28 - NR) (**Figure 7a**). Concerning progression-free survival (PFS), this score is able to predict also the patients in high and low risk with a with a log-rank p-value of 0.0067 (**Figure 7b**). The median PFS of low-risk patients is of 468 days (95% CI, 311 - NR), while high risk patients have a median PFS of 50 days (95% CI, 16 - NR).

Preprints (www.preprints.org) | NOT PEER-REVIEWED | Posted: 11 July 2022 doi:10.20944/preprints202207.0162.v1

Figure 7. Prognostic value of the ceRNA signature **7a)** Association of the ceRNA Risk score based on gene expression levels with overall survival in cutaneous metastatic melanoma. **7b)** Stratification of the patients according to PFS using the ceRNA-based risk score

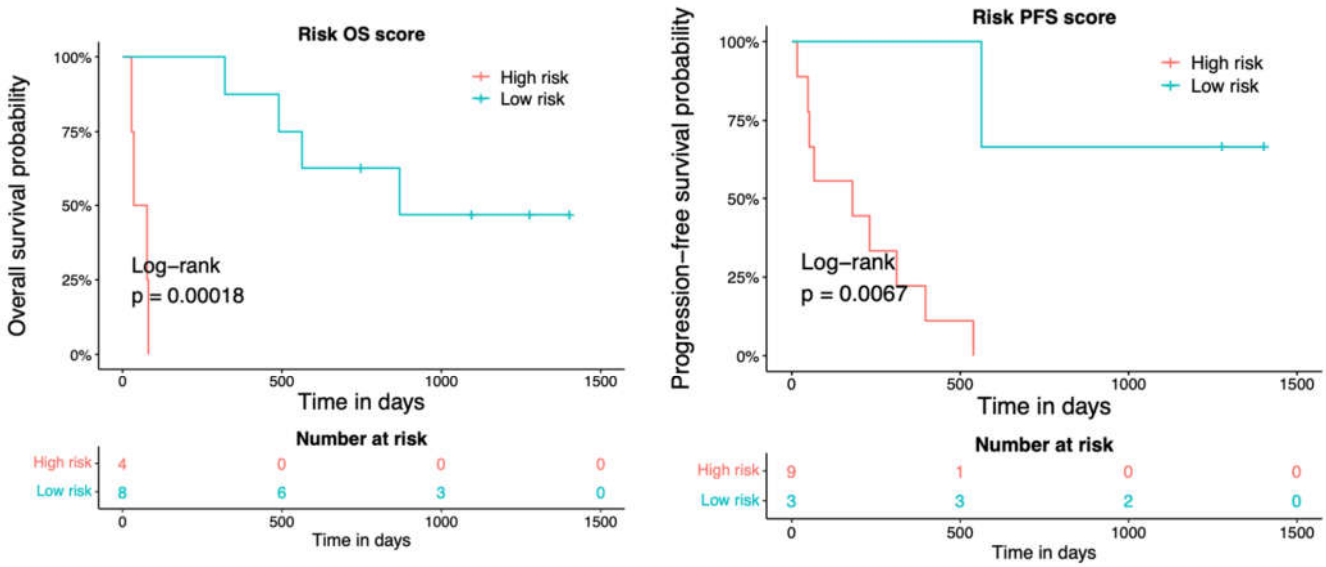

 doi:10.20944/preprints202207.0162.v1

4. Discussion

At present, the continuous improvement of high-throughput transcriptome sequencing technology and the increasingly complete gene bank data provide a powerful basis for the understanding of the transcriptomic reprogramming of immune cells in response to cancer cells. This is of special importance for understanding complex processes in which disentangling the role of the different modulators is key. One of these scenarios is the interaction between metastatic cells and the tumor microenvironment in the context of resistance to ICB. We know now that the immune-phenotype of the patients is strongly associated to the antitumoral effect of ICB drugs [64]. However, the regulation of this process has been scarcely explored.

In an attempt to unmask new players in the control of the ICB resistance mechanisms, we characterized the association of RNA species of recent annotation with the response to ICB in metastatic CM patients. CircRNAs and lncRNAs have recently gained considerable attention because of their potential implication in a wide range of cellular processes such as normal cell differentiation to tissue development and human illnesses [65] including melanoma etiology and therapy responses. Theses ncRNAs are normally considered to have pleiotropic effects, as they can affect a variety of pathways rather than acting primarily through a single target gene. In the specific context of CM, they have been reported to regulate the expression towards the growth and spread of CM cancer cells. This suggests a diagnostic and therapeutic target role for them[32] [66]. However, most of the current studies have focused on the differences in linear gene expression, while no one has addressed the specific influence of circular RNAs in response to ICB. Therefore, we performed transcriptome analysis of bulk metastatic melanoma tissue to generate information from both tumor and immune cells from the metastatic niche. Ribosomal-depleted RNA-seq provided us with information about circRNA, lncRNA and mRNA. Our strategy to discover the mechanisms associated with ICB resistance was to identify which circRNAs and lncRNAs were up or downregulated in the patients that were going to respond or not to the treatment. Next, we integrated them as regulatory layers in a network that included their putative mRNA targets that were also differentially expressed in good responders. In line with several previous reports that have paved the importance of immune function in the process of melanoma metastasis and ICB response [67], our results show a profound influence of the dysregulation of these ncRNAs on the activation or inhibition of key antitumor immunological processes such as the *Th1 pathway*, *Natural Killer Signaling*, *T cell receptor signaling* or the *PD-1, PD-L1 cancer immunotherapy* pathways. Interestingly, the expression perturbation of the good responders is associated with increasing expression of PD-1 and PD-L1 (CD274). The identification of these ncRNAs as regulators of PD-1 and PD-L1 expression is important for understanding the interindividual variation in this axis, which holds the first FDA approved marker for ICB [68]

We departed from the hypothesis that circRNAs and lncRNAs could regulate the response to ICB by exerting a sponge function that inhibited specific miRNAs as ceRNAs. In order to test this, we integrated the miRNAs that were both targets of the DE ceRNAs and targeting DE mRNAs of our dataset. The resulting selection of DE mRNAs targeted by those miRNAs was subjected to a correlation test with the ceRNAs. Consistently with our hypothesis, the expression correlations were always direct, suggesting that the increased expression of the ceRNAs was aligned with the increased expression of the mRNA putatively through inhibition of the corresponding miRNA. Since miRNAs expression information is absent from our dataset, our conclusions cannot include the direct association with the miRNAs.

On the other hand, the identification of the pattern of pathway aberration that was exclusive to the ceRNA-associated genes unmasked a modulatory role of the ceRNAs for a subset of specific resistance pathways. This finding implies that ceRNAs can either refine or oppose to the effects on the processes of drug response. This is particularly important for two pathways that are intrinsically related to the ICB response: *Natural Killer Cell Signaling* and *PD-1, PD-L1 cancer immunotherapy*. The dysregulation of the ceRNAs in good

 doi:10.20944/preprints202207.0162.v1

responders is related to the inhibition of the natural killer cells, while it ameliorates the inhibition of the PD-1/PD-L1 axis.

All in all, the major disruption of immunological antitumor pathways related to ceRNAs and observed in responders denote the crucial role that the tumor Immune microenvironment (TIME) plays in the treatment response to ICB. Some lines of evidence indicate that tumor cells can modify TIME by recruiting immunosuppressive cells and both circRNA and lncRNA are tools that tumor cells can use, via extravesicular particles, to get favorable TIME and in consequence leading to a treatment failure. Interestingly, previous reports, both in hepatocellular carcinoma and pancreatic cancer, associate specific cirRNA with response to targeted therapy and linked to NK cell dysregulation [69].

Two of the main molecules highlighted by the ceRNA network (Figure 5a) are TNF and IFNG. Recently, the overexpression of TNF, IFNG and IL2 among other molecules have been reported as key molecules that may enhance melanoma progression through activating the JAK-STAT signaling Pathway [70]. Moreover, other studies indicate that both TNF and IFNG are directly linked with high density and T cell infiltration and Cytotoxicity of cytotoxic T cells function (CTL) [71]. This process has been recently characterized by Weigelin et al, whose findings suggest that CTL-mediated apoptosis induction is not a one-size-fits-all process, and the most common mechanism of tumor cell eradication by antigen-specific CTL is the accumulation of sublethal damages [72]. Additionally, other studies had shown a strong positively correlation between TNF and PD-L1 expression and poor prognosis [73]. Based on our dataset, we speculate that some of the identified DE mRNAs of the TNF ligand family (*TNFSF8*, *TNFRSF9*, *TNFRSF17*, *TNFRSF13B*, *TNFRSF12A*, *TNFRSF11B*) (supplementary table 1) may affect the CTL activity and the lymphocyte infiltration. That supports the relevance of TNF in response to ICB in CCM and contributes to support the concept of combining therapies based on anti-TNF and anti-PD-1 in CMM.

With regards specific ceRNAs identified in this study, CDR1 circRNA stands out as potentially implementable biomarker of response. Previous studies have highlighted the relevance of CDR1 in cancer and particularly in the metastatic melanoma process. The main biological process identified to date is sponging miRNA-7, which is well established as a cancer progression marker. Recently, Hanniford, D et al described a more complex regulation of this region via the epigenetic silencing of the lncRNA *LINC00632* [20]. In our study, we have observed that CDR1 is one of the most relevant DE circRNAs, in terms of abundancy and differential expression in bad responders. Moreover, we observed that the good responders tend to have a more homogeneous CDR1 expression, indicating that CDR1 seems to be dysregulated in most of the bad responders. Further studies are needed to validate CDR1 for predicting and monitoring treatment response.

Finally, this work has found another utility as a generator of a prognosis prediction model in the context of response to ICB in metastatic CM. A prognostic Risk Score has been created for the signature of ceRNAs and used to stratify the patients in high and low risk for OS and PFS. The application of this score can be used to predict these outcomes. To our knowledge this the first time that a DE ceRNA signature could be associated to a prognosis of any ICB treatment.

In the current study, we have reported for the first time the association of circular RNAs with the response to immunotherapy. Together with specific lncRNAs, a new role for ncRNAs as ceRNA has been unmasked in the regulation of specific resistance mechanisms to ICB. The joint circRNA and lncRNA predictive signature has been used as well to build a prognosis score that reinforces the utility of these ncRNAs in the management of metastatic CM patients. All in all, this work provides a novel insight into the modulators of ICB resistant and imply the existence of new players to be considered as prognosis biomarkers and targets to counteract resistance in ICB treated cutaneous melanoma.

5. Conclusions

 doi:10.20944/preprints202207.0162.v1

In the present study, we have characterized the ceRNAs in metastatic melanoma patients treated with ICB to explore the biological role of ceRNA network on the response. Our exploratory analysis revealed that ceRNAs can modulate specific ICB resistance processes and therefore need to be considered in the complex regulatory scenario of the TIME interactions. Finally, the definition of a Risk Score based on the ceRNA expression signature constitutes a potentially useful tool for predicting prognosis in the context of ICB treatment in metastatic CM.

Supplementary Materials: The following are available online at www.mdpi.com/xxx/s1, Figure S1: title, Table S1: title, Video S1: title.

Author Contributions: JO and IB established the scientific hypothesis, IB, JO and JLO performed the study design, M G, AF, AL, EP-R, MC, MB, EA, AR and IB contributed to the cohort and clinical data collection, and generation and analysis of the results. JO, JLO, and IB were responsible for the composition of the manuscript.

Funding: The work is funded by Instituto de Salud Carlos III through the projects PI18/01592 (and FI19-00112 (to ALI) (Co-funded by the European Regional Development Fund/European Social Fund "A way to make Europe"/"Investing in your future"), Sistema Andaluz de Salud, through the projects SA 0263/2017, Nicolás Monardes (to IB) and PI-0121-2020, Spanish Group of Melanoma (Award for Best Research Project 2020) (to IB), Fundación Bancaria Unicaja through the project C19048 (to IB, MC), and Andalusia-Roche Network Mixed Alliance in Precision Medical Oncology (to IB, EA) and Consejeria de Salud PI-0121-2020 (to IB), RH0090-2020 CSYF 2020 (to JO)

Institutional Review Board Statement: In this section, you should add the Institutional Review Board Statement and approval number, if relevant to your study. You might choose to exclude this statement if the study did not require ethical approval. Please note that the Editorial Office might ask you for further information. Please add "The study was conducted according to the guidelines of the Declaration of Helsinki and approved by the Institutional Review Board (or Ethics Committee) of NAME OF INSTITUTE (protocol code XXX and date of approval)." OR "Ethical review and approval were waived for this study, due to REASON (please provide a detailed justification)." OR "Not applicable" for studies not involving humans or animals.

Informed Consent Statement: Informed consent was obtained from all subjects involved in the study.

Data Availability Statement: Please refer to suggested Data Availability Statements in section "MDPI Research Data Policies" at https://www.mdpi.com/ethics.

Acknowledgments: We thank Ms. Martina Alvarez, Vanessa de Luque and Ms. Cynthia Robles (Medical Oncology Unit Intercentros) for assistance in patients sample extraction and processing.

Conflicts of Interest: The authors declare no conflict of interest

Appendix A

Preprints (www.preprints.org) | NOT PEER-REVIEWED | Posted: 11 July 2022 doi:10.20944/preprints202207.0162.v1

Supplementary figure 1. Exon type of circRNA. Mapping of circRNA indicates that 98,3% of circRNA identified are exon-exon type.

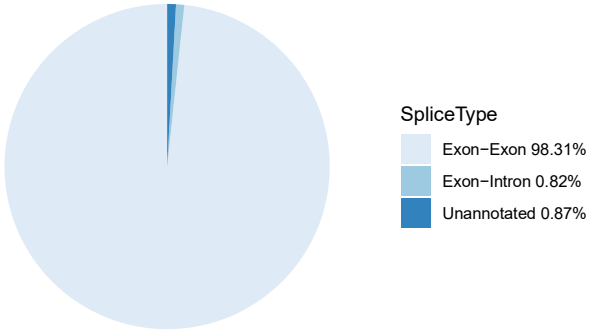

Supplementary figure 2**. Radial graphic of networks merged by IPA of the main DEmRNA of ceRNA pinpointing the central role of TNF.**

Preprints (www.preprints.org) | NOT PEER-REVIEWED | Posted: 11 July 2022 doi:10.20944/preprints202207.0162.v1

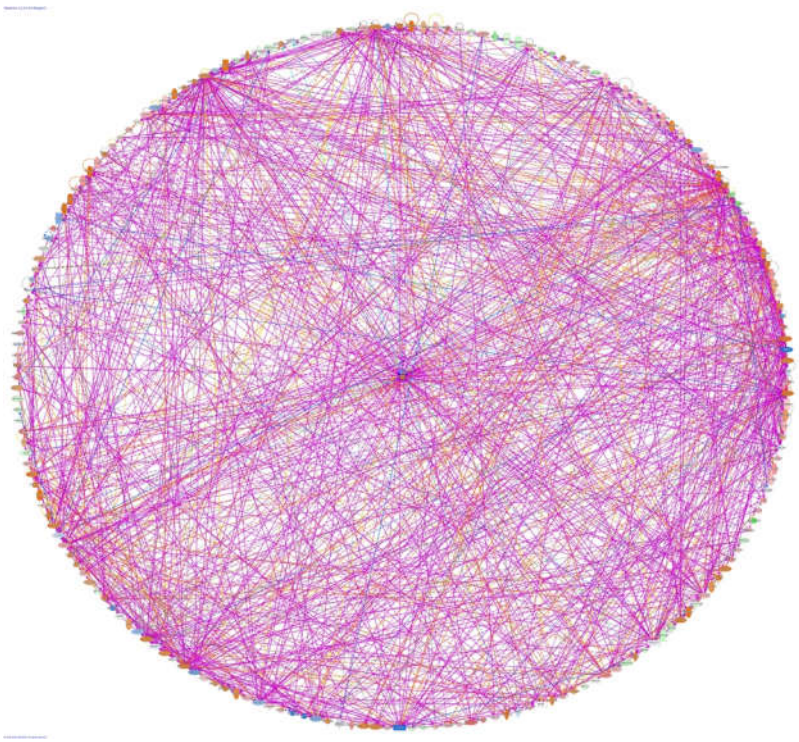

Supplementary figures 4. Figure **4a)**. Interaction networks of the main molecules of the DEmRNA of ceRNA predicted by IPA. Figure **4b)**. Relevant upstream molecules indicates the activation cascades of IL27 EBI3 and the inhibition of SAFB

a)

Preprints (www.preprints.org) | NOT PEER-REVIEWED | Posted: 11 July 2022 doi:10.20944/preprints202207.0162.v1

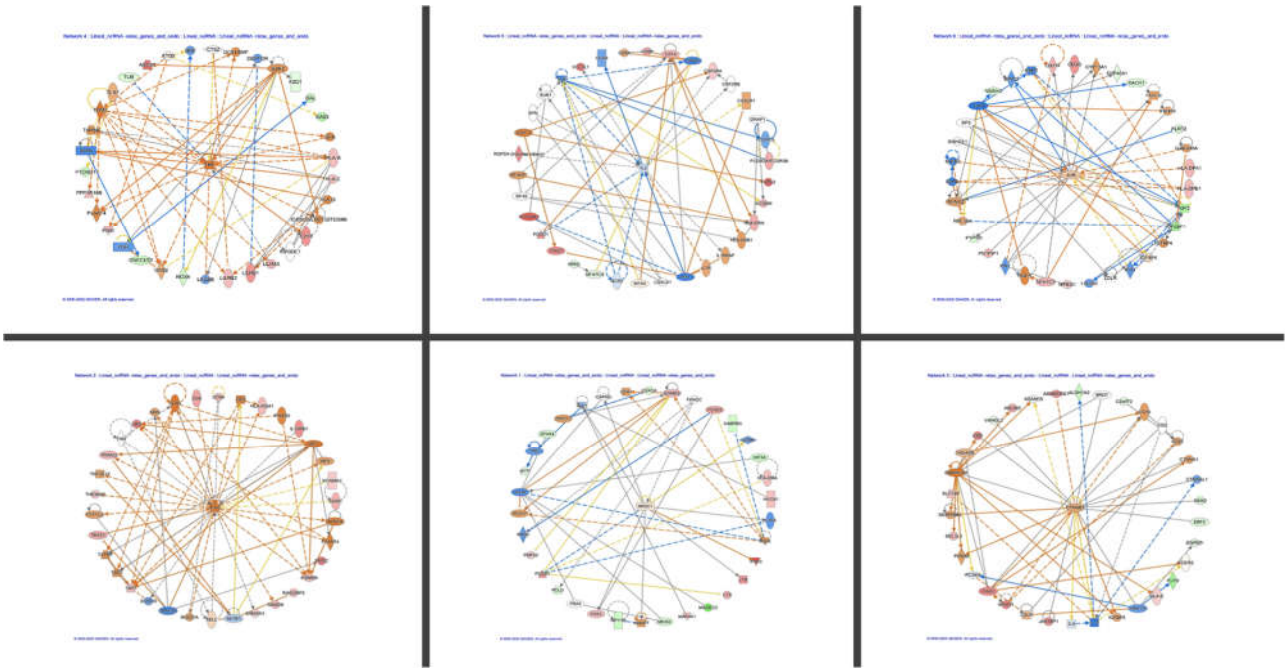

b)

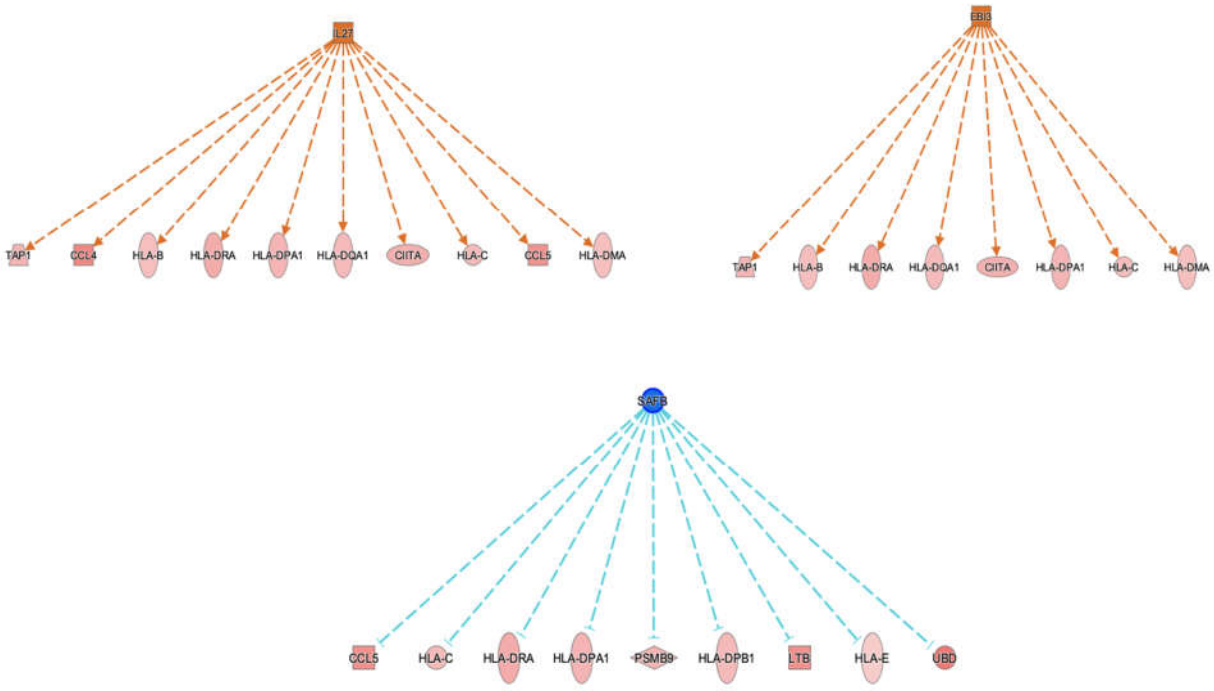

 doi:10.20944/preprints202207.0162.v1

References

1. Shakhova, O. Neural Crest Stem Cells in Melanoma Development. *Current Opinion in Oncology* **2014**, *26*, 215–221, doi:10.1097/cco.0000000000000046.
2. Wang, J.X.; Fukunaga-Kalabis, M.; Herlyn, M. Crosstalk in Skin: Melanocytes, Keratinocytes, Stem Cells, and Melanoma. *Journal of Cell Communication and Signaling* 2016, *10*, 191–196.
3. Erdei, E.; Torres, S.M. A New Understanding in the Epidemiology of Melanoma. *Expert Review of Anticancer Therapy* 2010, *10*, 1811–1823.
4. Ferlay J, Laversanne M, Ervik M, Lam F, Colombet M, Mery L, Piñeros M, Znaor A, Soerjomataram I, B.F. Global Cancer Observatory: Cancer Tomorrow Available online: https://gco.iarc.fr/tomorrow (accessed on 9 March 2022).
5. Sung, H.; Ferlay, J.; Siegel, R.L.; Laversanne, M.; Soerjomataram, I.; Jemal, A.; Bray, F. Global Cancer Statistics 2020: GLOBOCAN Estimates of Incidence and Mortality Worldwide for 36 Cancers in 185 Countries. *CA: A Cancer Journal for Clinicians* **2021**, caac.21660, doi:10.3322/caac.21660.
6. Martens, M.C.; Seebode, C.; Lehmann, J.; Emmert, S. Photocarcinogenesis and Skin Cancer Prevention Strategies: An Update. *Anticancer Research* 2018, *38*, 1153–1158.
7. Hodis, E.; Watson, I.R.; Kryukov, G. V.; Arold, S.T.; Imielinski, M.; Theurillat, J.P.; Nickerson, E.; Auclair, D.; Li, L.; Place, C.; et al. A Landscape of Driver Mutations in Melanoma. *Cell* **2012**, *150*, 251–263, doi:10.1016/J.CELL.2012.06.024.
8. Palmieri, G.; Ombra, M.; Colombino, M.; Casula, M.; Sini, M.; Manca, A.; Paliogiannis, P.; Ascierto, P.A.; Cossu, A. Multiple Molecular Pathways in Melanomagenesis: Characterization of Therapeutic Targets. *Frontiers in Oncology* **2015**, *5*, 1, doi:10.3389/FONC.2015.00183.
9. Damsky, W.E.; Bosenberg, M. Melanocytic Nevi and Melanoma: Unraveling a Complex Relationship. *Oncogene 2017 36:42* **2017**, *36*, 5771–5792, doi:10.1038/onc.2017.189.

10. Ding, L.; Kim, M.; Kanchi, K.L.; Dees, N.D.; Lu, C.; Griffith, M.; Fenstermacher, D.; Sung, H.; Miller, C.A.; Goetz, B.; et al. Clonal Architectures and Driver Mutations in Metastatic Melanomas. *PLOS ONE* **2014**, *9*, e111153, doi:10.1371/JOURNAL.PONE.0111153.
11. Vergara, I.A.; Mintoff, C.P.; Sandhu, S.; McIntosh, L.; Young, R.J.; Wong, S.Q.; Colebatch, A.; Cameron, D.L.; Kwon, J.L.; Wolfe, R.; et al. Evolution of Late-Stage Metastatic Melanoma Is Dominated by Aneuploidy and Whole Genome Doubling. *Nature Communications 2021 12:1* **2021**, *12*, 1–15, doi:10.1038/s41467-021-21576-8.
12. Larkin, J.; Chiarion-Sileni, V.; Gonzalez, R.; Grob, J.-J.; Rutkowski, P.; Lao, C.D.; Cowey, C.L.; Schadendorf, D.; Wagstaff, J.; Dummer, R.; et al. Five-Year Survival with Combined Nivolumab and Ipilimumab in Advanced Melanoma. *New England Journal of Medicine* **2019**, *381*, 1535–1546, doi:10.1056/nejmoa1910836.
13. Sharma, P.; Hu-Lieskovan, S.; Wargo, J.A.; Ribas, A. Primary, Adaptive, and Acquired Resistance to Cancer Immunotherapy. *Cell* 2017, *168*, 707–723.
14. Aldea, M.; Andre, F.; Marabelle, A.; Dogan, S.; Barlesi, F.; Soria, J.-C. Overcoming Resistance to Tumor-Targeted and Immune-Targeted Therapies. *Cancer Discovery* **2021**, *11*, 874–899, doi:10.1158/2159-8290.CD-20-1638.
15. Gide, T.N.; Wilmott, J.S.; Scolyer, R.A.; Long, G. V. Primary and Acquired Resistance to Immune Checkpoint Inhibitors in Metastatic Melanoma. *Clinical Cancer Research* 2018, *24*, 1260–1270.
16. Filipovic, A.; Miller, G.; Bolen, J. Progress Toward Identifying Exact Proxies for Predicting Response to Immunotherapies. *Frontiers in Cell and Developmental Biology* 2020, *8*, 155.
17. Zhang, X.; Xie, K.; Zhou, H.; Wu, Y.; Li, C.; Liu, Y.; Liu, Z.; Xu, Q.; Liu, S.; Xiao, D.; et al. Role of Non-Coding RNAs and RNA Modifiers in Cancer Therapy Resistance. *Molecular Cancer* 2020, *19*, 1–26.
18. Chen, S.; Luo, L.; Chen, H.; He, C. The Current State of Research Regarding the Role of Non-Coding Rnas in Cutaneous Squamous Cell Carcinoma. *OncoTargets and Therapy* 2020, *13*, 13151–13158.
19. Hansen, T.B.; Jensen, T.I.; Clausen, B.H.; Bramsen, J.B.; Finsen, B.; Damgaard, C.K.; Kjems, J. Natural RNA Circles Function as Efficient MicroRNA Sponges. *Nature* **2013**, *495*, 384–388, doi:10.1038/nature11993.
20. Hanniford, D.; Ulloa-Morales, A.; Karz, A.; Berzoti-Coelho, M.G.; Moubarak, R.S.; Sánchez-Sendra, B.; Kloetgen, A.; Davalos, V.; Imig, J.; Wu, P.; et al. Epigenetic Silencing of CDR1as Drives IGF2BP3-Mediated Melanoma Invasion and Metastasis. *Cancer Cell* **2020**, *37*, 55-70.e15, doi:10.1016/j.ccell.2019.12.007.
21. Qian, P.; Linbo, L.; Xiaomei, Z.; Hui, P. Circ_0002770, Acting as a Competitive Endogenous RNA, Promotes Proliferation and Invasion by Targeting MiR-331-3p in Melanoma. *Cell Death and Disease* **2020**, *11*, doi:10.1038/s41419-020-2444-x.
22. W, L.; Y, S.; Z, Z.; Y, X.; J, W. CircRNA_0084043 Promote Malignant Melanoma Progression via MiR-153-3p/Snail Axis. *Biochem Biophys Res Commun* **2018**, *502*, 22–29, doi:10.1016/J.BBRC.2018.05.114.
23. Chen, Z.; Chen, J.; Wa, Q.; He, M.; Wang, X.; Zhou, J.; Cen, Y. Knockdown of Circ_0084043 Suppresses the Development of Human Melanoma Cells through MiR-429/Tribbles Homolog 2 Axis and Wnt/β-Catenin Pathway. *Life Sciences* **2020**, *243*, doi:10.1016/j.lfs.2020.117323.
24. Bian, D.; Wu, Y.; Song, G. Novel Circular RNA, Hsa_circ_0025039 Promotes Cell Growth, Invasion and Glucose Metabolism in Malignant Melanoma via the MiR-198/CDK4 Axis. *Biomedicine and Pharmacotherapy* **2018**, *108*, 165–176, doi:10.1016/j.biopha.2018.08.152.
25. Jin, C.; Dong, D.; Yang, Z.; Xia, R.; Tao, S.; Piao, M. CircMYC Regulates Glycolysis and Cell Proliferation in Melanoma. *Cell Biochemistry and Biophysics* **2020**, *78*, 77–88, doi:10.1007/s12013-019-00895-0.
26. Lu, J.; Li, Y. Circ_0079593 Facilitates Proliferation, Metastasis, Glucose Metabolism and Inhibits Apoptosis in Melanoma by Regulating the MiR-516b/GRM3 Axis. *Molecular and Cellular Biochemistry* **2020**, *475*, 227–237, doi:10.1007/s11010-020-03875-8.

27. Tian, S.; Han, G.; Lu, L.; Meng, X. Circ-FOXM1 Contributes to Cell Proliferation, Invasion, and Glycolysis and Represses Apoptosis in Melanoma by Regulating MiR-143-3p/FLOT2 Axis. *World Journal of Surgical Oncology* **2020**, *18*, doi:10.1186/s12957-020-01832-9.
28. Wei, C.Y.; Zhu, M.X.; Lu, N.H.; Liu, J.Q.; Yang, Y.W.; Zhang, Y.; Shi, Y.D.; Feng, Z.H.; Li, J.X.; Qi, F.Z.; et al. Circular RNA Circ_0020710 Drives Tumor Progression and Immune Evasion by Regulating the MiR-370-3p/CXCL12 Axis in Melanoma. *Molecular Cancer* **2020**, *19*, doi:10.1186/s12943-020-01191-9.
29. Mecozzi, N.; Vera, O.; Karreth, F.A. Squaring the Circle: CircRNAs in Melanoma. *Oncogene* 2021, *40*, 5559–5566.
30. Montico, B.; Giurato, G.; Pecoraro, G.; Salvati, A.; Covre, A.; Colizzi, F.; Steffan, A.; Weisz, A.; Maio, M.; Sigalotti, L.; et al. The Pleiotropic Role of Circular and Long Noncoding RNAs in Cutaneous Melanoma. *Molecular Oncology* 2021.
31. Tang, K.; Zhang, H.; Li, Y.; Sun, Q.; Jin, H. Circular RNA as a Potential Biomarker for Melanoma: A Systematic Review. *Frontiers in Cell and Developmental Biology* **2021**, *0*, 696, doi:10.3389/FCELL.2021.638548.
32. Melixetian, M.; Pelicci, P.G.; Lanfrancone, L. Regulation of LncRNAs in Melanoma and Their Functional Roles in the Metastatic Process. *Cells* 2022, *11*.
33. Chen, L.; Zhang, Y.H.; Pan, X.; Liu, M.; Wang, S.; Huang, T.; Cai, Y.D. Tissue Expression Difference between Mrnas and Lncrnas. *International Journal of Molecular Sciences* **2018**, *19*, doi:10.3390/ijms19113416.
34. Tay, Y.; Rinn, J.; Pandolfi, P.P. The Multilayered Complexity of CeRNA Crosstalk and Competition. *Nature* 2014, *505*, 344–352.
35. Xu, T.; Wang, M.; Jiang, L.; Ma, L.; Wan, L.; Chen, Q.; Wei, C.; Wang, Z. CircRNAs in Anticancer Drug Resistance: Recent Advances and Future Potential. *Molecular Cancer* 2020, *19*.
36. Zhang, C.; Ding, R.F.; Sun, Y.C.; Huo, S.T.; He, A.; Wen, C.; Chen, H.H.; Du, W.W.; Lai, W.N.; Wang, H. Circular RNA in Tumor Metastasis. *Molecular Therapy - Nucleic Acids* 2021, *23*, 1243–1257.
37. Gao, Y.; Wang, J.; Zhao, F. CIRI: An Efficient and Unbiased Algorithm for de Novo Circular RNA Identification. *Genome Biology* **2015**, *16*, 1–16, doi:10.1186/s13059-014-0571-3.
38. Zhang, X.O.; Dong, R.; Zhang, Y.; Zhang, J.L.; Luo, Z.; Zhang, J.; Chen, L.L.; Yang, L. Diverse Alternative Back-Splicing and Alternative Splicing Landscape of Circular RNAs. *Genome Research* **2016**, *26*, 1277–1287, doi:10.1101/gr.202895.115.
39. Cheng, J.; Metge, F.; Dieterich, C. Specific Identification and Quantification of Circular RNAs from Sequencing Data. *Bioinformatics* **2016**, *32*, 1094–1096, doi:10.1093/bioinformatics/btv656.
40. Akers, N.K.; Schadt, E.E.; Losic, B. STAR Chimeric Post for Rapid Detection of Circular RNA and Fusion Transcripts. *Bioinformatics* **2018**, *34*, 2364–2370, doi:10.1093/bioinformatics/bty091.
41. Zhang, J.; Chen, S.; Yang, J.; Zhao, F. Accurate Quantification of Circular RNAs Identifies Extensive Circular Isoform Switching Events. *Nature Communications* **2020**, *11*, doi:10.1038/s41467-019-13840-9.
42. Wu, W.; Ji, P.; Zhao, F. CircAtlas: An Integrated Resource of One Million Highly Accurate Circular RNAs from 1070 Vertebrate Transcriptomes. *Genome Biology* **2020**, *21*, 1–14, doi:10.1186/s13059-020-02018-y.
43. Mas-Ponte, D.; Carlevaro-Fita, J.; Palumbo, E.; Pulido, T.H.; Guigo, R.; Johnson, R. LncATLAS Database for Subcellular Localization of Long Noncoding RNAs. *Rna* **2017**, *23*, 1080–1087, doi:10.1261/rna.060814.117.
44. Lin, Y.C.; Lee, Y.C.; Chang, K.L.; Hsiao, K.Y. Analysis of Common Targets for Circular RNAs. *BMC Bioinformatics* **2019**, *20*, 1–6, doi:10.1186/s12859-019-2966-3.
45. Kozomara, A.; Birgaoanu, M.; Griffiths-Jones, S. MiRBase: From MicroRNA Sequences to Function. *Nucleic Acids Research* **2019**, *47*, D155–D162, doi:10.1093/nar/gky1141.
46. Enright, A.J.; John, B.; Gaul, U.; Tuschl, T.; Sander, C.; Marks, D.S. MicroRNA Targets in Drosophila. *Genome Biol* **2003**, *5*, 1–14, doi:10.1186/GB-2003-5-1-R1/TABLES/6.

47. Paraskevopoulou, M.D.; Vlachos, I.S.; Karagkouni, D.; Georgakilas, G.; Kanellos, I.; Vergoulis, T.; Zagganas, K.; Tsanakas, P.; Floros, E.; Dalamagas, T.; et al. DIANA-LncBase v2: Indexing MicroRNA Targets on Non-Coding Transcripts. *Nucleic Acids Research* **2016**, *44*, D231–D238, doi:10.1093/nar/gkv1270.
48. Ru, Y.; Kechris, K.J.; Tabakoff, B.; Hoffman, P.; Radcliffe, R.A.; Bowler, R.; Mahaffey, S.; Rossi, S.; Calin, G.A.; Bemis, L.; et al. The MultiMiR R Package and Database: Integration of MicroRNA-Target Interactions along with Their Disease and Drug Associations. *Nucleic Acids Research* **2014**, *42*, e133, doi:10.1093/nar/gku631.
49. Maragkakis, M.; Vergoulis, T.; Alexiou, P.; Reczko, M.; Plomaritou, K.; Gousis, M.; Kourtis, K.; Koziris, N.; Dalamagas, T.; Hatzigeorgiou, A.G. DIANA-MicroT Web Server Upgrade Supports Fly and Worm MiRNA Target Prediction and Bibliographic MiRNA to Disease Association. *Nucleic Acids Research* **2011**, *39*, W145, doi:10.1093/NAR/GKR294.
50. Gaidatzis, D.; van Nimwegen, E.; Hausser, J.; Zavolan, M. Inference of MiRNA Targets Using Evolutionary Conservation and Pathway Analysis. *BMC Bioinformatics* **2007**, *8*, 1–22, doi:10.1186/1471-2105-8-69.
51. Griffiths-Jones, S.; Saini, H.K.; Van Dongen, S.; Enright, A.J. MiRBase: Tools for MicroRNA Genomics. *Nucleic Acids Research* **2008**, *36*, doi:10.1093/nar/gkm952.
52. Betel, D.; Wilson, M.; Gabow, A.; Marks, D.S.; Sander, C. The MicroRNA.Org Resource: Targets and Expression. *Nucleic Acids Research* **2008**, *36*, doi:10.1093/nar/gkm995.
53. Wang, X. MiRDB: A MicroRNA Target Prediction and Functional Annotation Database with a Wiki Interface. *RNA* **2008**, *14*, 1012–1017, doi:10.1261/rna.965408.
54. Blin, K.; Dieterich, C.; Wurmus, R.; Rajewsky, N.; Landthaler, M.; Akalin, A. DoRiNA 2.0-Upgrading the Dorina Database of RNA Interactions in Post-Transcriptional Regulation. *Nucleic Acids Research* **2015**, *43*, D160–D167, doi:10.1093/nar/gku1180.
55. Akbari Moqadam, F.; Pieters, R.; Den Boer, M.L. The Hunting of Targets: Challenge in MiRNA Research. *Leukemia* 2013, *27*, 16–23.
56. Grimson, A.; Farh, K.K.H.; Johnston, W.K.; Garrett-Engele, P.; Lim, L.P.; Bartel, D.P. MicroRNA Targeting Specificity in Mammals: Determinants beyond Seed Pairing. *Molecular Cell* **2007**, *27*, 91–105, doi:10.1016/j.molcel.2007.06.017.
57. Yao, D.; Zhang, L.; Zheng, M.; Sun, X.; Lu, Y.; Liu, P. Circ2Disease: A Manually Curated Database of Experimentally Validated CircRNAs in Human Disease. *Scientific Reports* **2018**, *8*, 1–6, doi:10.1038/s41598-018-29360-3.
58. Rophina, M.; Sharma, D.; Poojary, M.; Scaria, V. Circad: A Comprehensive Manually Curated Resource of Circular RNA Associated with Diseases. *Database* **2020**, *2020*, 19, doi:10.1093/DATABASE/BAAA019.
59. Xia, S.; Feng, J.; Chen, K.; Ma, Y.; Gong, J.; Cai, F.; Jin, Y.; Gao, Y.; Xia, L.; Chang, H.; et al. CSCD: A Database for Cancer-Specific Circular RNAs. *Nucleic Acids Research* **2018**, *46*, D925–D929, doi:10.1093/nar/gkx863.
60. QIAGEN Inc. Ingenuity Pathway Analysis (IPA) Available online: https://www.qiagen.com/us/products/discovery-and-translational-research/next-generation-sequencing/informatics-and-data/interpretation-content-databases/ingenuity-pathway-analysis/ (accessed on 30 September 2021).
61. Gu, Z.; Eils, R.; Schlesner, M. Complex Heatmaps Reveal Patterns and Correlations in Multidimensional Genomic Data. *Bioinformatics* **2016**, *32*, 2847–2849, doi:10.1093/bioinformatics/btw313.
62. Wickham, H. *Ggplot2*; Springer New York, 2009;
63. Wang, W.; Zhu, D.; Zhao, Z.; Sun, M.; Wang, F.; Li, W.; Zhang, J.; Jiang, G. RNA Sequencing Reveals the Expression Profiles of CircRNA and Identifies a Four-CircRNA Signature Acts as a Prognostic Marker in Esophageal Squamous Cell Carcinoma. *Cancer Cell International* **2021**, *21*, 1–14, doi:10.1186/S12935-021-01852-9/FIGURES/6.

64. Petitprez, F.; Meylan, M.; de Reyniès, A.; Sautès-Fridman, C.; Fridman, W.H. The Tumor Microenvironment in the Response to Immune Checkpoint Blockade Therapies. *Frontiers in Immunology* **2020**, *11*, doi:10.3389/FIMMU.2020.00784/FULL.
65. López-Jiménez, E.; Andrés-León, E. The Implications of Ncrnas in the Development of Human Diseases. *Noncoding RNA* 2021, *7*.
66. Montico, B.; Giurato, G.; Pecoraro, G.; Salvati, A.; Covre, A.; Colizzi, F.; Steffan, A.; Weisz, A.; Maio, M.; Sigalotti, L.; et al. The Pleiotropic Roles of Circular and Long Noncoding RNAs in Cutaneous Melanoma. *Molecular Oncology* 2022, *16*, 565–593.
67. Marzagalli, M.; Ebelt, N.D.; Manuel, E.R. Unraveling the Crosstalk between Melanoma and Immune Cells in the Tumor Microenvironment. *Seminars in Cancer Biology* **2019**, *59*, 236–250, doi:10.1016/J.SEMCANCER.2019.08.002.
68. Wang, Y.; Tong, Z.; Zhang, W.; Zhang, W.; Buzdin, A.; Mu, X.; Yan, Q.; Zhao, X.; Chang, H.-H.; Duhon, M.; et al. FDA-Approved and Emerging Next Generation Predictive Biomarkers for Immune Checkpoint Inhibitors in Cancer Patients. *Article* **2021**, *11*, 1, doi:10.3389/fonc.2021.683419.
69. Carlos-Reyes, Á.; Romero-Garcia, S.; Contreras-Sanzón, E.; Ruiz, V.; Prado-Garcia, H. Role of Circular RNAs in the Regulation of Immune Cells in Response to Cancer Therapies. *Frontiers in Genetics* 2022, *13*.
70. Zhang, C.; Dang, D.; Cong, L.; Sun, H.; Cong, X. Pivotal Factors Associated with the Immunosuppressive Tumor Microenvironment and Melanoma Metastasis. *Cancer Medicine* **2021**, *10*, 4710–4720, doi:10.1002/CAM4.3963.
71. Garbe, C.; Krasagakis, K. Effects of Interferons and Cytokines on Melanoma Cells. *Journal of Investigative Dermatology* **1993**, *100*, S239–S244, doi:10.1038/JID.1993.83.
72. Weigelin, B.; den Boer, A.T.; Wagena, E.; Broen, K.; Dolstra, H.; de Boer, R.J.; Figdor, C.G.; Textor, J.; Friedl, P. Cytotoxic T Cells Are Able to Efficiently Eliminate Cancer Cells by Additive Cytotoxicity. *Nature Communications* **2021**, *12*, doi:10.1038/S41467-021-25282-3.
73. Bertrand, F.; Montfort, A.; Marcheteau, E.; Imbert, C.; Gilhodes, J.; Filleron, T.; Rochaix, P.; Andrieu-Abadie, N.; Levade, T.; Meyer, N.; et al. TNFα Blockade Overcomes Resistance to Anti-PD-1 in Experimental Melanoma. *Nature Communications 2017 8:1* **2017**, *8*, 1–13, doi:10.1038/s41467-017-02358-7.